



# Field measurement of microclimate of sunken square and its effect on indoor environment of underground metro station in subtropical region



Jianjian Zhao<sup>a,b</sup>, Jiankai Dong<sup>a,b</sup>, Xiaohai Zhang<sup>a,b</sup>, Yanling Na<sup>c,d</sup>, Chongxu Jiang<sup>c,d</sup>, Feng He<sup>e</sup>, Qijie Cui<sup>e</sup>, Jing Liu<sup>a,b,\*</sup>

<sup>a</sup> School of Architecture, Harbin Institute of Technology, Harbin, 150000, China

<sup>b</sup> Key Laboratory of Cold Region Urban and Rural Human Settlement Environment Science and Technology, Ministry of Industry and Information Technology, Harbin, 150000, China

<sup>c</sup> China Railway Design Corporation, Tianjin, 300308, China

<sup>d</sup> National Engineering Laboratory for Digital Construction and Evaluation Technology of Urban Rail Transit, Tianjin, 300308, China

<sup>e</sup> China Railway Design Corporation, Southern China Branch, Shenzhen, 518000, China

## ARTICLE INFO

### Keywords:

Microclimate  
Sunken square  
Underground metro station  
Thermal comfort  
Indoor environment

## ABSTRACT

Because of the needs of rail transit and urban construction, metro stations have various forms of entrances. In particular, in recent years, the sunken square has been increasingly designed and applied to underground transportation hub systems. Because the sunken square is directly connected to the indoor environment through the entrances, the microclimate of the sunken square can directly affect the indoor environment. When air enters the underground transportation hub through the entrance, it has a nonnegligible impact on indoor thermal comfort and energy consumption. In this study, two representative metro stations with sunken squares in Shenzhen, China, which is a typical metropolis in a subtropical region, were selected. The microclimates of the sunken squares were investigated, the air flow rates through the entrances were measured, and the indoor environments of the two stations were studied. The test results show that the attenuation effect of wind increases with the shape coefficient of the sunken squares. In addition, the temperature gradually increases from the bottom to the top of the sunken square. The neutral physiological equivalent temperature (PET) in the sunken squares was 29 and 19 °C in summer and winter, respectively. Meanwhile, the air flow rate through the sunken square entrances was relatively large, and the influence factor was obtained. The results of the systematic measurements provide a data basis and technical guidance for the design of sunken squares and metro stations, and can help improve the quality of the indoor environment in such underground metro stations.

## 1. Introduction

The development of rail transit is an important part of the urbanisation process. As an important urban transportation tool, metro railway systems have developed rapidly in recent years [1,2]. According to the Union International des Transports Publics (UITP) report of global metro statistics, ridership data show that, on average, approximately 168 million passengers use the metro network in 182 cities within 56 countries on a regular basis, and the annual ridership through metro stations worldwide is as much as 54 billion [3,4]. Fifty-one cities had opened and operated 272 urban rail transit lines, with an operating mileage of 8819 km, in China by 2021 [5]. It is increasingly important to study the indoor thermal environment and air quality in metro stations

because they greatly affect the health and comfort of people [6–8].

The entrances are the areas where the internal environment of the metro station connects with the outdoor environment. With the development of the metro railway system and to meet different needs, the forms of entrances are gradually becoming diversified. The entrances of the metro station are divided into three forms, as shown in Fig. 1: independent entrances directly connected to the outdoors by stairs, composite entrances shared with shopping centres or other commercial buildings, and sunken square entrances connected to the sunken square and then transitioning to the outdoors. Independent and composite entrances are common forms in urban metro stations. However, the entrances of the metro station must meet the requirements of the convenience of passengers and the safety requirements for evacuation. Moreover, with the emergence of urban transit-oriented development

\* Corresponding author. School of Architecture, Harbin Institute of Technology, Harbin, 150000, China.

E-mail address: [liujinghit0@163.com](mailto:liujinghit0@163.com) (J. Liu).

## Nomenclature

$A_i$	area of the large opening of entrances, m <sup>2</sup>
$D$	hydraulic radius of the bottom surface, m
$D_g$	black globe radius, m
$H$	height of the sunken square, m
$N$	number of sunken square entrances
$n$	air exchange rate of the metro station, h <sup>-1</sup>
$Q_s$	air flow rate of sunken square entrances, m <sup>3</sup> /h
$Q_{s,in}$	air flow rate of metro station from outdoors to indoors through sunken square entrances, m <sup>3</sup> /h
$T_a$	air temperature, °C
$T_g$	black globe temperature, °C
$T_{mrt}$	mean radiation temperature, °C
$V$	volume of the metro station, m <sup>3</sup>
$v_i$	average hourly wind speed at sunken square entrances, m/s
$v_o$	wind speed of background weather parameter, m/s
$v_s$	wind speed of the sunken square, m/s
$\varepsilon$	absorption rate of black globe
$\omega$	shape coefficient of the sunken square

square is the integration of multiple functions, such as commerce, entertainment, and leisure. It not only improves the urban environment but also gives people a new urban space experience. Compared with other forms of entrances, the sunken square entrances have many special advantages. They are conducive to the use of three-dimensional multi-functional composite space, improve the ventilation and lighting of the underground space, and blur the feelings of being above ground and underground, thereby improving the quality of the space [13].

Because the sunken square entrances are connected to the external environment through the sunken square space, outdoor air can easily enter the underground metro station through the entrances from the sunken square, which has an impact on indoor thermal comfort and energy consumption. Some studies have been carried out on the influence of entrances on the air movement and indoor environment in metro stations [14–20]; however, there have been few studies focusing on on-site measurements and quantifying the effects of the sunken squares and entrances on the thermal environment and air flow in underground metro stations. Guan et al. [14] found that the outdoor air intake through entrances was enormous and played an important role in the outdoor air supply. Hong and Kim [15] studied the energy consumption of a metro station in Korea and concluded that the number of entrances affects energy consumption because the outdoor air enters freely through the entrances. In addition, some studies have used computational fluid dynamics and wind tunnel methods to study the ventilation

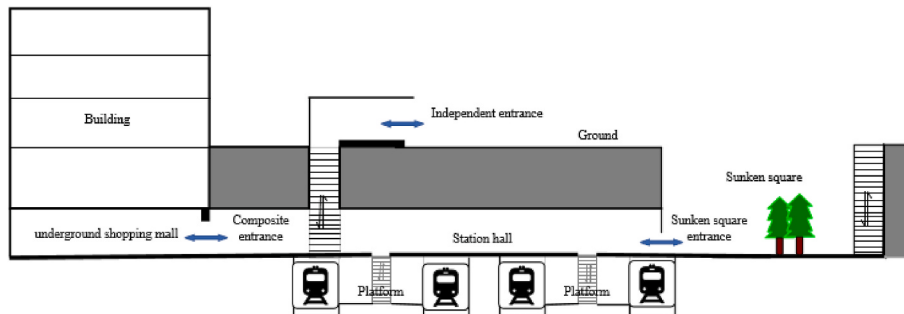


Fig. 1. Schematic diagram of different forms of metro station entrances.

(TOD) theory (TOD guides the design of metro station complexes, is conducive to the efficient use of urban resources, and promotes the integrated development of the station and city) [9–12], metro stations with the characteristics of semi-opening and the sunken square entrances are becoming increasingly popular. The advantage of the sunken

characteristics of entrances. Liu et al. [21] studied the ventilation of an independent entrance of a typical metro station based on numerical simulations and experiments, and the air flow of the independent entrance was investigated. The above research mainly focused on the independent entrances. In a study by Di et al. [22], the wind speed of the

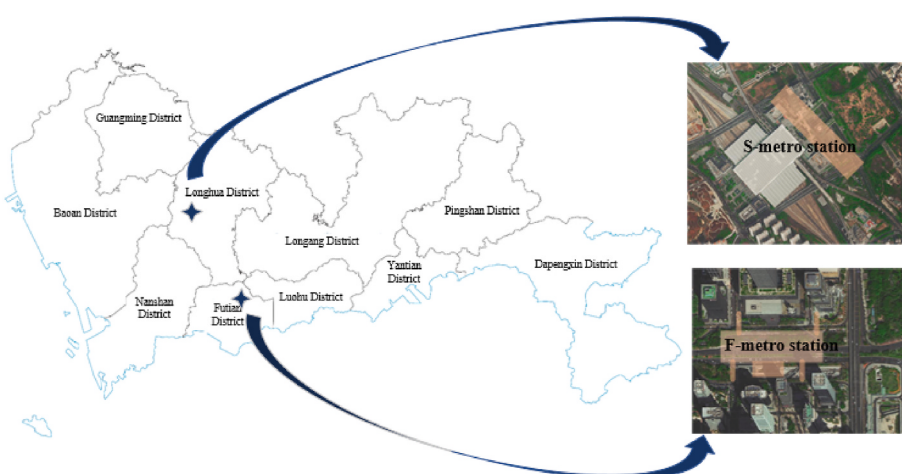


Fig. 2. Location of the metro stations in Shenzhen.

**Table 1**

Details of the two metro stations.

	F-metro station	S-metro station
Station area	66,383 m <sup>2</sup>	182,074 m <sup>2</sup>
Station depth	29 m	18 m
Number of entrances	9 (8 independent and 1 sunken square)	6 (2 independent and 4 sunken square)
Metro lines	Lines 3, 5, and 11	Lines 4, 5, and 6
Forms of platforms	6 side platforms	2 side and 2 island platforms

sunken square was less than the outdoor wind speed. Gang et al. [23] used ENVI-met software to simulate the microclimate of a sunken square, revealing that combining sunshade, a green wall, and water can reduce the temperature by as much as 5.6 °C in a sunken square. Therefore, it is important to study the microclimates of sunken squares and the air flow characteristics of underground metro stations with sunken square entrances.

In this study, two representative metro stations with sunken squares in Shenzhen, China, which is a typical metropolis in a subtropical region, were selected. The microclimates of the sunken squares and the air flow rates through the entrances were measured. The influences of sunken squares on the indoor environment and the thermal comfort of passengers in the sunken squares of the two stations were also studied. Through the test of two underground metro station in Shenzhen, the general rule of the influence of the sunken square on the underground metro station is obtained. The results provide a data basis and technical guidance for the design of sunken squares and metro stations, and can help improve the quality of the indoor environment in such underground metro stations.

## 2. Description of field test sites

This study was conducted at the Futian and Shenzhen North metro stations (hereinafter referred to as 'F-metro station' and 'S-metro station', respectively), which are located in Shenzhen, China. The locations of the metro stations are shown in Fig. 2. Shenzhen is a coastal city in southern China, located at longitude 113°46' to 114°37' east and latitude 22°27' to 22°52' north, and it is a typical subtropical area. Shenzhen has 12 metro lines and an operating mileage of 546 km as of 2022 [24].

The F-metro station is the largest transportation hub interchange station located in Futian district. It is a three-level underground station and connects to three metro lines: Lines 3, 5, and 11. The S-metro station is located in Longhua district. It is also a large-scale comprehensive transportation hub for regional passenger transportation with port functions. It is an interchange station for Lines 4, 5, and 6, and the platform of Line 5 is located on the underground floor and has a side platform. The details of the two stations are shown in Table 1. These two metro stations use the same form of air conditioning and ventilation. In winter and transition seasons, the underground metro stations adopt mechanical ventilation to supply fresh air, and the fresh air unit is fully turned on and the air-conditioning system is turned off. In summer, the air-conditioning system runs, the supply air temperature is 18 °C, and the minimum fresh air mode is turned on to send in an appropriate amount of fresh air to save energy and meet the demand for fresh air.

The sunken squares at the two metro stations have different characteristics. The sunken square of the F-metro station has a size of 43 m (L) × 13.8 m (W) × 12 m (H), and the ground of sunken square is covered with dark tiles and planted with green shrubs. The sunken square of the S-metro station is equipped with a large fountain pool with glass at the bottom and has an internal skylight, and the size of the sunken square is 57 m (L) × 46 m (W) × 12 m (H). The fountain pool is 30 m (L) × 28 m (W), and the depth of the water was approximately 0.5

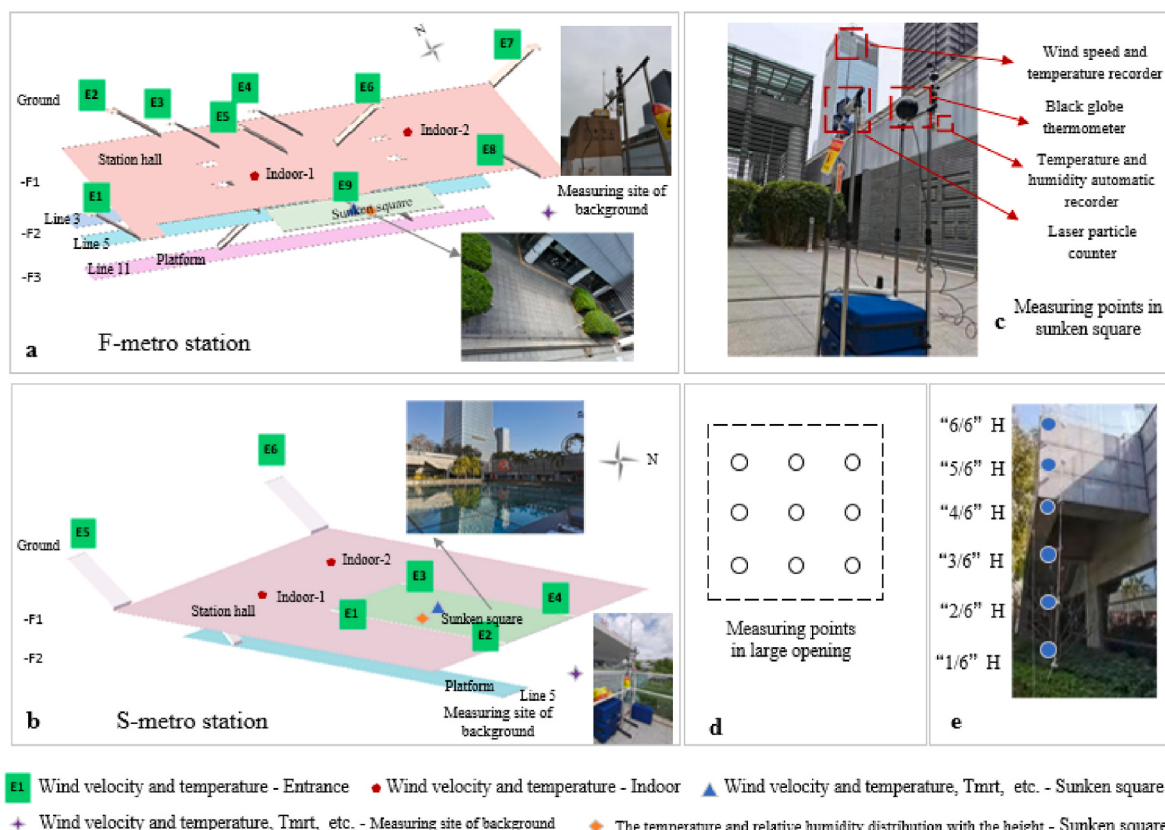


Fig. 3. Schematic diagram of the underground metro stations and the implementation of the field experiments.

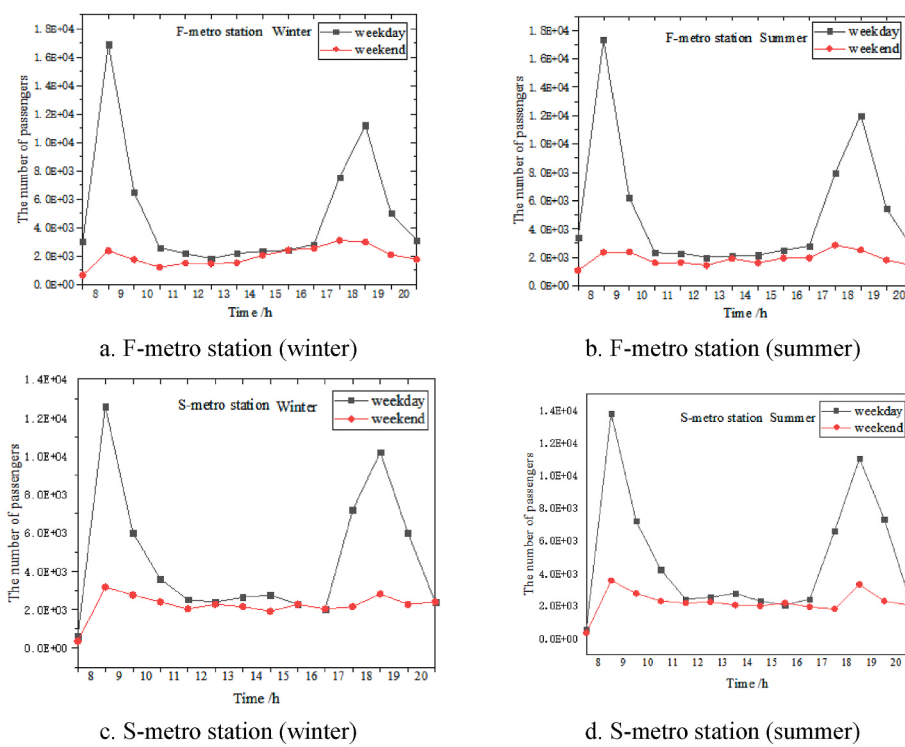


Fig. 4. Number of passengers using the metro stations in different seasons.

m during the test period. The ground is covered with dark tiles, and green hardwood trees and shrubs are planted inside. The pictures of the sunken squares are shown in Fig. 3a and b.

### 3. Methodology

#### 3.1. Field test methods and instruments

To measure the microclimates of the sunken squares, air flows through the entrances, and indoor environments of the two stations, January and July were selected as the representative months of winter and summer, respectively. The entire measurement period was from 9 to 15 January (winter) and from 14 to 22 July (summer) in 2021. The measurement time was 8:00–20:00 every day. The test time period includes representative time nodes, such as the morning and evening rush hours. The passenger flow was acquired by the automatic fare collection system set up at the entrances of the station hall where passengers enter and exit the metro station. Fig. 4 shows the average number of passengers on weekdays and weekends during the test period. On weekdays, there are two obvious peaks during rush hours: 8:00–9:00 and 18:00–19:00. There is no obvious peak period on the weekend, when the passenger flow distribution is relatively even. Due to the obvious rush

hour on weekdays, the passenger flow on weekdays is much larger than that on weekends. The total number of passengers on weekdays is 2–2.7 times that on weekends. It should be noted that the number of transfer passengers is not considered in this study due to the limitations of testing methods. Because this study mainly focuses on the microclimate of the sunken square and the fluctuation of passenger flow is only used as the research background data, we believe that the lack of transit passenger flow data could not affect the correctness of the research conclusions.

#### 3.1.1. Measurements of the sunken square microclimate

To study the characteristics of the sunken square microclimate, the thermal environment parameters of the sunken squares were tested. The instruments for the tests were arranged in the centres of the sunken squares. The measuring sites are shown in Fig. 3a and b. The instruments used for testing were mounted on self-made instrument stands, as shown in Fig. 3c. The position was 1.5 m from the ground of the sunken square. The test parameters were the temperature, relatively humidity, wind speed, black globe temperature, and particle concentration. Moreover, the temperature and relatively humidity distribution characteristics were tested along the height of the sunken squares. Six measuring sites were arranged along the height within the sunken squares, as shown in Fig. 3e. To test the internal wall and ground temperature distributions of

**Table 2**

Information about the measurement devices.

Measurement parameter	Measurement site	Instrument name	Equipment type	Intervals	Operational range	Accuracy
Temperature, Relative humidity	Entrances, indoors, sunken square, background weather parameters	Temperature and humidity automatic recorder	HOBO pro U23-002	300 s	-20–70 °C	0.1 °C, 2% RH
Air velocity, temperature	Entrances, indoors, sunken square, background weather parameters	Wind speed and temperature recorder	WFWZY-1	60 s	0.05–30 m/s -20–80 °C	5% ± 0.05 m/s, ±0.5 °C
Particle concentration	Sunken square, background weather parameters	Laser particle counter	TSI-8533	60 s	0.3–25 um	0.3 μm > 50%, >0.45 μm, 100%
Smoking pen	Entrances	Wind direction	-	-	-	-
Black globe temperature	Sunken square, background weather parameters	Black globe thermometer	HQZY-1	60 s	-40–60 °C	±0.3 °C
Surface temperature	Sunken square	Thermal infrared imager	Ti480PRO	1 h	-10–1000 °C	±2 °C or 2%

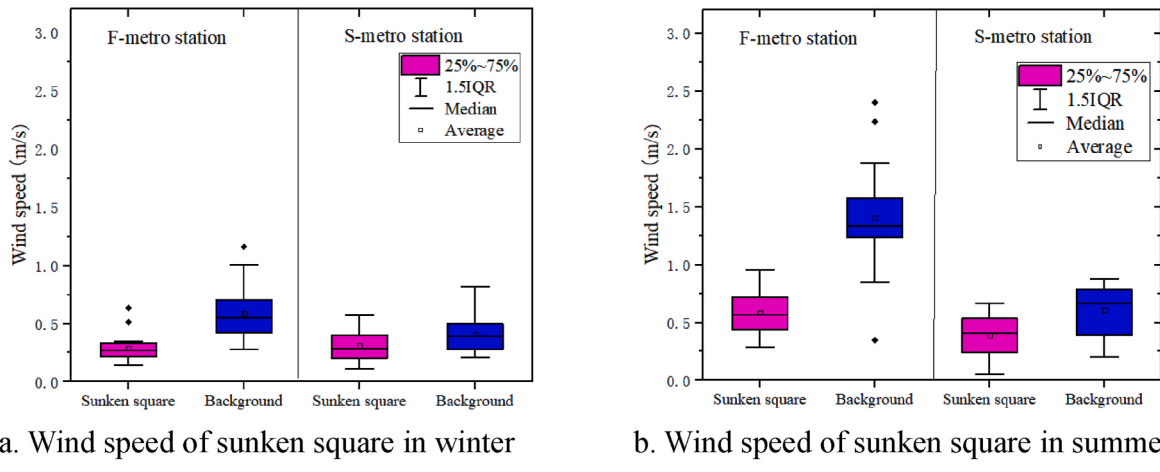


Fig. 5. Wind speed of sunken square in different seasons.

the sunken squares, infrared cameras (Fluke infrared thermal imager) were also used to record the temperature distributions inside the sunken squares. Meanwhile, the measurement site of the background meteorological parameters outside the sunken squares were set up in F-metro station and S-metro station respectively as shown in Fig. 3a. The area near the measurement site of the background meteorological parameters in the two station is different and the S-metro station is sheltered by buildings, resulting in differences in meteorological parameters. Therefore, it is necessary to test the background meteorological parameters of the two stations separately. Self-made instrument stands were placed at a height of 1.5 m above the ground. The test parameters were the temperature, relatively humidity, wind speed, wind direction, solar radiation, and particle concentration. The detailed information of the test instruments is provided in Table 2.

### 3.1.2. Measurements of air flow rate entering metro station through the entrances of sunken squares and indoor environment

To estimate the air flow rate entering the station through the entrances of the sunken squares, the wind speeds were automatically recorded by the wind speed and temperature recorders, and a recording interval of 10 s was set. Meanwhile, nine measuring points were arranged evenly at the large openings of the entrances [25,26], as shown in Fig. 3d. And smoking pen was used to record the wind direction at the large openings of the entrances when the wind speed was tested with the wind speed and temperature recorders.

To study the influence of air flow through the entrances on the indoor environment, the temperature and wind speed at the metro stations were tested. Indoor measuring points were set up in the F-metro station and S-metro station. The measuring point height was at the pedestrian height of 1.5 m to test the indoor wind speed and temperature, and the sites of the measuring points are shown in the Fig. 3a and b. The detailed information of the test instruments is shown in Table 2.

### 3.1.3. Estimation method of the air flow rate

According to the measurement of the wind speed of the large opening of the entrances, the air flow rates of the sunken square entrances of the metro stations are estimated according to Eq. (1).

$$Q_s = \pm 3600 \cdot \sum_{i=1}^N v_i \cdot A_i \quad (1)$$

where  $Q_s$  is the air flow rate of metro station sunken square entrances ( $\text{m}^3/\text{h}$ ), '+' represents the wind direction from outdoors to indoors, '-' represents the wind direction from indoors to outdoors,  $N$  is the number of sunken square entrances (in the F-metro station,  $N = 1$ , the sunken square entrance is E9, as shown in Fig. 3; in the S-metro station,  $N = 4$ ,

the sunken square entrances are E1–E4),  $v_i$  is the hourly average wind speed of the  $i$  sunken square entrances ( $\text{m}/\text{s}$ ), and  $A_i$  is the area of the large opening of the  $i$  sunken square entrances ( $\text{m}^2$ ) (in the F-metro station,  $A_i$  is  $8.25 \text{ m}^2$ ; in the S-metro station,  $A_i$  is  $7.5 \text{ m}^2$ ).

The air exchange rates of the sunken square entrances of the metro stations are estimated according to Eq. (2).

$$n = \frac{Q_{s,in}}{V} \quad (2)$$

where  $Q_{s,in}$  is the air flow rate of the metro station from outdoors to indoors through the sunken square entrances ( $\text{m}^3/\text{h}$ ),  $n$  is the air exchange rate of the metro station through the sunken square entrances ( $\text{h}^{-1}$ ), and  $V$  is the volume of the metro station ( $\text{m}^3$ ).

## 3.2. Questionnaire survey and evaluation index of thermal comfort

### 3.2.1. Questionnaire design

A questionnaire survey was used to investigate the thermal sensation, thermal comfort, and other conditions in the sunken square. In this study, the questionnaire was divided into two parts. The first part involves the personal information (gender, age), clothing, activity status, and activity purpose of the subjects. The second part is the thermal sensation vote (TSV), thermal comfort vote (TCV), and acceptability vote of the subjects. In this study, the TSV was rated on a seven-point scale (i.e., -3, 'very cold'; -2, 'cold'; -1, 'cool'; 0, 'neutral'; 1, 'warm'; 2, 'hot'; 3, 'very hot') [27,28]. The TCV also used a seven-point scale (i.e., -3, 'very uncomfortable'; -2, 'uncomfortable'; -1, 'slightly uncomfortable'; 0, 'neutral'; 1, 'slightly comfortable'; 2, 'comfortable'; 3, 'very comfortable') [29]. Moreover, the questionnaire contained a question regarding the health condition of the subject aimed to prevent subjects from filling out the questionnaire when they were unhealthy.

### 3.2.2. Physiological equivalent temperature

The thermal comfort index physiological equivalent temperature (PET) [30] was used in this study because the PET is considerably more sensitive to wind speed and solar radiation [31] and is more suitable for outdoor thermal comfort assessment than predicted mean voting and standardised effective temperature [32]. PET can be calculated as the air temperature at which the energy balance for the assumed indoor conditions ( $T_{mrt}$  = mean radiation temperature, vapor pressure  $p_v = 12 \text{ hPa}$ ,  $v = 0.1 \text{ m/s}$ ) is balanced with the same mean skin temperature and sweat rate as calculated for the actual outdoor conditions. In this study, the PET was calculated with Rayman software [33–35]. The  $T_{mrt}$  parameter [36], which was necessary to calculate the PET, was estimated by Eq. (3) and in accordance with the ISO 7726 standard.

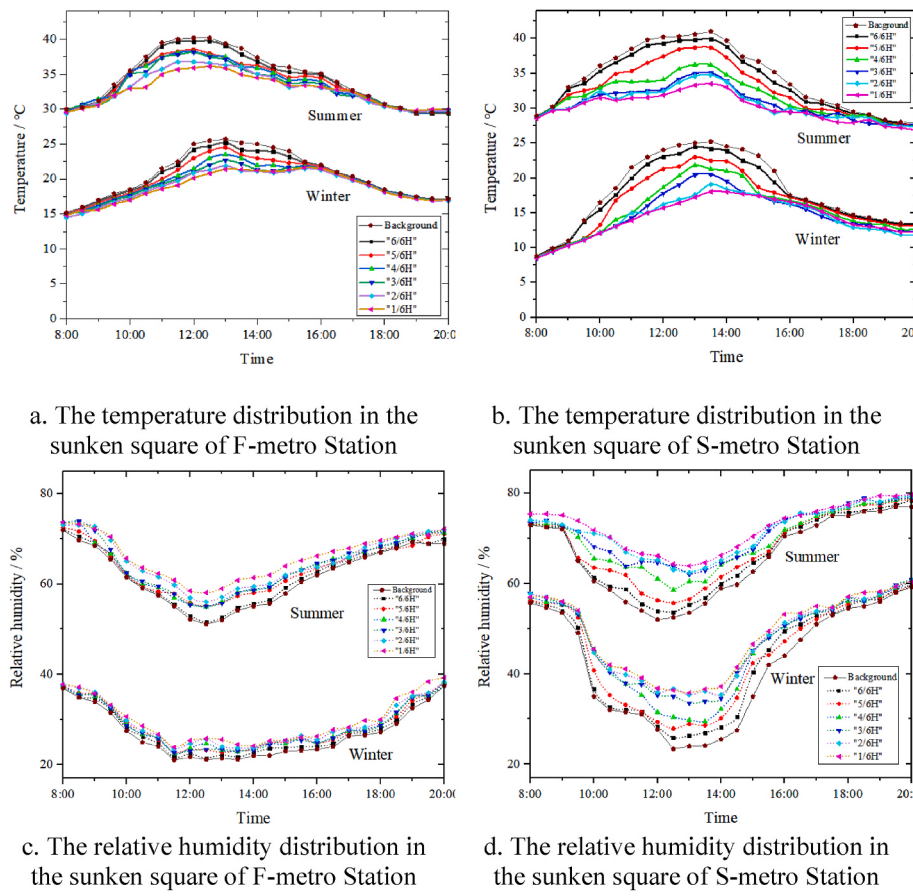


**Fig. 6.** Temperature and relative humidity with the change in height in the sunken square.

$$T_{mrt} = \left[ (T_g + 273.15)^4 + \frac{1.10 \cdot 10^8 v_s^{0.6}}{\varepsilon D_g^{0.4}} (T_g - T_a) \right]^{1/4} - 273.15 \quad (3)$$

where  $T_{mrt}$  is the mean radiation temperature ( $^{\circ}\text{C}$ ),  $T_g$  and  $T_a$  are the black globe temperature and air temperature, respectively ( $^{\circ}\text{C}$ ),  $v_s$  is the wind speed in the sunken square (m/s),  $D_g$  is the sphere diameter (m, a standard black globe is used and the diameter is 0.15 m), and  $\varepsilon$  is the emissivity of the sphere (a value of 0.95 is used for a black globe in this study).

#### 4. Field measurement results

##### 4.1. Microclimate of the sunken square

###### 4.1.1. Wind speed in the sunken square

In the field measurement, the hourly average wind speed in the sunken square and background weather parameter were obtained and analysed. The hourly average wind speed in the sunken square and background in the F-metro and S-metro stations according to the statistical results are as shown in Fig. 5. The background wind speeds at the different metro stations differed even when the measurement was carried out simultaneously. At both metro stations, the average wind speed in the sunken square was significantly lower than the corresponding wind speed of the background weather parameter, indicating that the sunken square has an attenuation effect on the wind speed of the background weather parameter. The ratio of the average wind speed of the sunken square to the wind speed of background weather parameter at the F-metro station was 2 in winter and 2.3 in summer, whereas it was larger than 1.3 in winter and 1.6 in summer at the S-metro station. The difference in ratio is related to the shape coefficient of the sunken

square, which is discussed in detail in Section 5.1.

###### 4.1.2. Temperature and relative humidity distribution with height in the sunken square

Fig. 6a and b shows the daily average temperature distribution with the change in height in the sunken square of the F-metro and S-metro stations, respectively, during the measurement period. The temperature gradually increased from the bottom (1/6H) to the top (6/6H) of the sunken square. Moreover, the temperature difference was not large until 9:00 in the morning. Over time, the temperature difference increased. The maximum temperature difference occurred around 12:30–13:30; after 14:00, the temperature difference gradually decreased. Because of the sheltering effect of the walls and plants of the sunken square, the internal temperature of the sunken square was lower than the temperature of the background weather parameter. In addition, the temperature difference in the S-metro station sunken square was larger than that of the F-metro station sunken square. In winter, the maximum temperature difference of 1/6H and 6/6H was as much as 4  $^{\circ}\text{C}$  in the F-metro station sunken square and 5.2  $^{\circ}\text{C}$  in the S-metro station sunken square. In summer, the maximum temperature difference of 1/6H and 6/6H was 4.5  $^{\circ}\text{C}$  in the F-metro station sunken square and 6.4  $^{\circ}\text{C}$  in the S-metro station sunken square. For the temperature difference of the sunken squares and background weather parameter, the difference was larger than the difference of 1/6H and 6/6H; for example, in summer, the maximum temperature difference of 1/6H and the background was 5.2  $^{\circ}\text{C}$  in the F-metro station sunken square and 7.2  $^{\circ}\text{C}$  in the S-metro station sunken square. The reason was that the evaporation and heat absorption of the fountain pool and the sheltering effect of trees in the S-metro station sunken square made the temperature lower than that of the F-metro station sunken square. Moreover, in summer, the sunken square had a

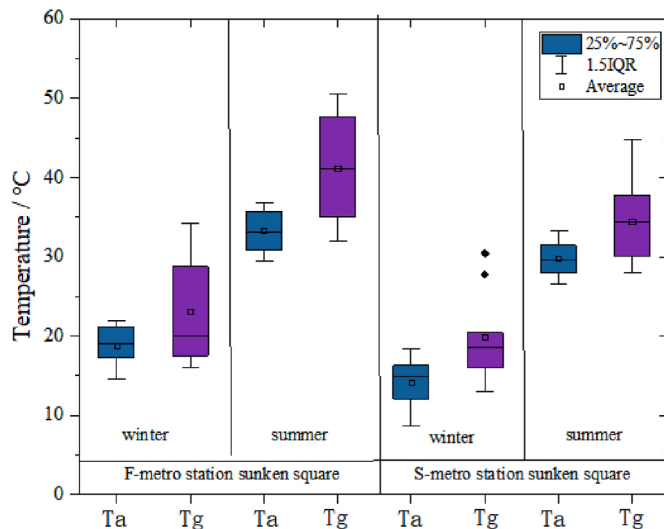


**Fig. 7.** Air temperature and black globe temperature of the sunken square.

more obvious shielding effect on solar radiation. The vertical temperature difference in the sunken square was greater in summer than in winter because of the stronger solar radiation in summer.

Fig. 6c and d shows the daily average relative humidity distribution with the change in height in the sunken square of the F-metro and S-metro stations, respectively. The relative humidity of the sunken square gradually decreased with height. Moreover, the difference in relative humidity in the vertical measurement site increased first and then decreased, and it reached the maximum value around 12:30–14:00. In the sunken square of the F-metro station, the average relative humidity difference of 1/6H and 6/6H was 3.6% in winter and 5.7% in summer. However, in the sunken square of the S-metro station, the average relative humidity difference of the 1/6H and 6/6H was 9.6% in winter and 12.8% in summer. For the relative humidity difference of the sunken squares and the background weather parameter, the difference was also larger than the difference of 1/6H and 6/6H; for example, in summer, the maximum relative humidity difference of 1/6H and the background was 6% in the F-metro station sunken square and 15% in the S-metro station sunken square. The difference in relative humidity is more obvious in the S-metro station sunken square than in the F-metro station sunken square, primarily because of the transpiration of trees and shrubs and the fountain pond in the sunken square, in addition to the influence of temperature.

#### 4.1.3. Air temperature and black globe temperature of the sunken square

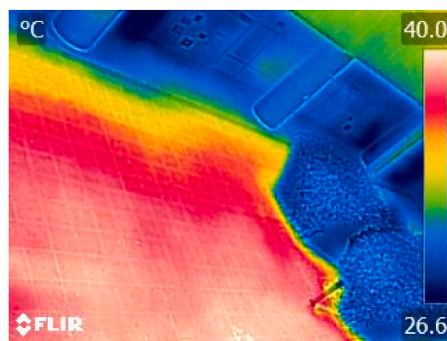
The air temperature ( $T_a$ ) and black globe temperature ( $T_g$ ) of the two sunken squares are shown in Fig. 7. In winter, the average  $T_a$  was 4.6 °C higher in the F-metro station sunken square than that of the S-metro station sunken square. In summer, the average  $T_a$  in the F-metro station sunken square was 3 °C higher than that of the S-metro station sunken square. In addition, the water body in the S-metro station sunken square had a strong solar radiation absorption effect and also a strong heat storage capacity, as shown in Fig. 8. The maximum temperature on the ground of the F-metro station sunken square was up to 40.1 °C, which was significantly larger than the maximum temperature of 33.7 °C in the S-metro station sunken square.

#### 4.1.4. Concentration of particulate matter in the sunken square

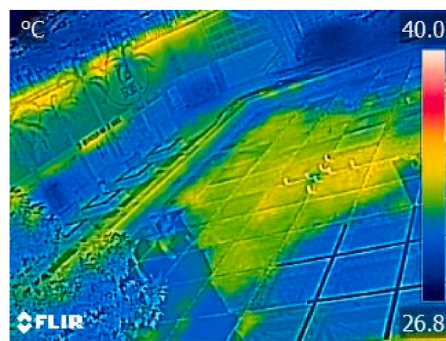
Fig. 9 shows the hourly average distribution of the concentration of particles of 0.3–0.5, 0.5–1.0, 1.0–5.0, 5.0–10.0, and >10.0  $\mu\text{m}$  in the sunken square and the background parameter. In general, there is a good linear correlation of the concentration of particles between the sunken square and background parameter. In addition, the sunken square particle concentration in all particle size ranges is greater than the background particle concentration because the wind attenuated in the sunken square, as shown in Fig. 5, leading to the accumulation of particulate matter [23]. The range of the ratio of the different-size-particle concentration of the sunken square to the background parameter was 1.2–2.7 in the F-metro station sunken square, whereas, in S-metro station sunken square, it was 1.05–2.2, which was consistent with the previous comparison of the wind speed ratios of the two stations. Moreover, the ratio of the concentration of particles with a larger particle size of the sunken square to the background parameter was higher than for a smaller particle size. Therefore, the ratio increases with the particle size because the sedimentation effect of the particles with a larger size is more obvious in the sunken square.

#### 4.1.5. Questionnaire TSV and TCV results

During the measurement, 402 questionnaires were collected in F-metro station and 419 questionnaires were collected in S-metro station, respectively. In F-metro station, the ratio of males to females was 56%–44%. Among the questionnaire respondents, 47% were under the age of 30, 32% were between 30 and 40, and 21% were older than 40. And in S-metro station, the ratio of males to females was 51%–49%. Among the questionnaire respondents, 40% were under the age of 30, 35% were between 30 and 40, and 25% were older than 40. The TSVs and TCVs for passengers in the questionnaire are shown in the Fig. 10. In winter, the TSVs were mainly distributed over ‘neutral’ and ‘slightly cool’. The most frequently perceived thermal sensation was ‘neutral’ in the two sunken squares. However, the ‘neutral’ thermal sensation in the F-metro station sunken square was 52.9%, which was more than the 46.1% in the S-



a. Temperature distribution of wall and floor surface of F-metro station sunken square (13:00)



b. Temperature distribution of wall and floor surface of S-metro station sunken square (13:00)

**Fig. 8.** Temperature distribution of wall and floor surface of sunken square in summer.

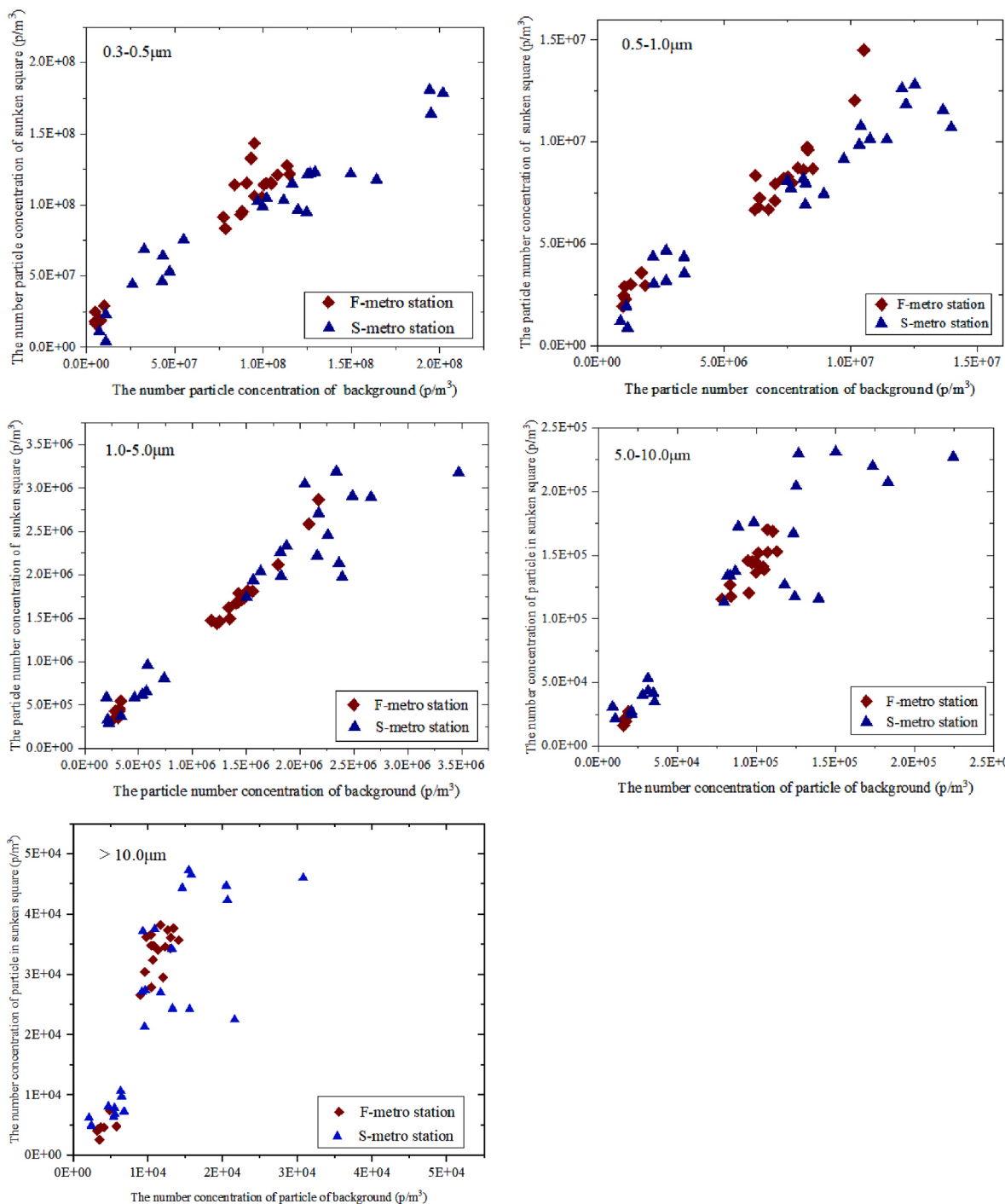


**Fig. 9.** Relationship between particle concentration of the sunken square and background parameter.

metro station sunken square. The reason is that the temperature was higher in the F-metro station sunken square than in the S-metro station. In summer, all votes were higher than 0 (neutral). The most frequently perceived TSV was 'hot' in two sunken squares. Furthermore, 9% and 5% of the votes were 'very hot' in the F-metro and S-metro station sunken squares, respectively.

For both sunken squares, the voting rate on the uncomfortable side ( $TCV < 0$ ) in summer was higher than that in winter. This is thought to be a consequence of a large percentage of 'hot' and 'very hot' votes in summer. In summer, the uncomfortable side ( $TCV < 0$ ) in the F-metro station sunken square was 87%, whereas it was 73% in the S-metro station sunken square. The reason is that the cooling effect of the

fountain pool in sunken square improved the thermal comfort. In winter, the uncomfortable side ( $TCV < 0$ ) in the F-metro station sunken square was 37.9%, which was still larger than 29% for the S-metro station sunken square. Even the  $TSV = 0$  ('neutral') vote in the F-metro station sunken square was larger than that for the S-metro station sunken square. The reason is believed to be that the high wind speed in the F-metro station sunken square reduced the thermal comfort.

#### 4.2. Influence of sunken square on the metro station environment

**Fig. 11a** and **b** shows the wind speed distribution at the F-metro and S-metro stations, respectively. In general, the wind speeds of the sunken

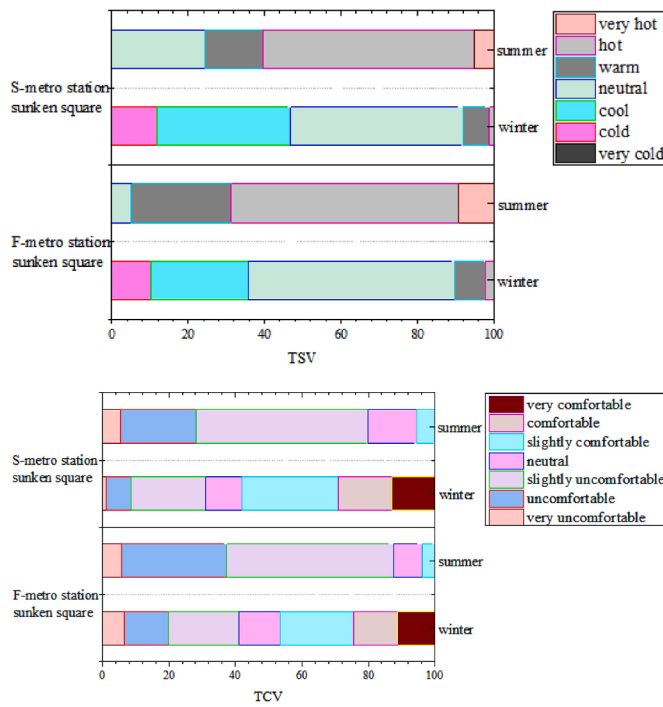


**Fig. 10.** Questionnaire result of TSV and TCV.

square entrances were larger than for the indoor environment and independent entrances. The wind speeds of the sunken square entrances were 3.2–9.1 times higher than those of the independent entrances. This is because the outdoor air enters the indoor environment in different ways. In the independent entrance, the wind must enter through the escalator or stairs, so the resistance increases because of the attenuation effect of the stairs on the wind [21]. In the sunken square entrances, the wind can enter directly through the large openings with less resistance. Meanwhile, the wind speed at the sunken square entrances is larger in winter than in summer. The reason is that the indoor temperature was higher than background temperature in winter, and the buoyancy effect of the air was more likely to cause an exchange of indoor and outdoor air. The wind speed at the sunken square entrances of the F-metro station was higher than that of the S-metro station sunken square, which was possibly related to the relative positions and numbers of entrances in the sunken squares.

Fig. 11c and d shows the temperature distributions at the F-metro and S-metro stations. The indoor temperature distribution of different measuring points is not uniform. In summer, the average temperature of the entrances was 2–3.2 °C higher than that of the indoor environment in the two metro stations. This was caused by the air flow through the entrances. Moreover, the temperature near the independent entrance was 1.2–2.5 °C higher than the temperature of the sunken square entrance. The reason is that the warmer background air directly entered the indoor environment at the independent entrances, whereas, in the sunken square entrances, the local cooling effect of the sunken square made the air temperature entering the room lower than the background. In winter, the temperature at the entrances of the sunken square was significantly lower than the indoor temperature, whereas the temperature near the independent entrances differed little from the indoor temperature because the wind speed of the sunken square entrances was large, making the temperature difference from the indoor environment obvious. Moreover, the indoor temperature of the S-metro station hall was significantly higher than that of F-metro station, which was related to the number of sunken square entrances at the S-metro station. However, the indoor air temperature was lower than that of the F-metro station hall in winter.

## 5. Discussion

### 5.1. Shape coefficient of the sunken square

To analyse the influence of the shape and size of the sunken square on the air flow, the shape coefficient of the sunken square, defined as Eq. (4), is used. The definition of the corresponding variables is shown in Fig. 12. The relationship between the hourly average wind speed of the background and sunken square is shown in Fig. 13. There is a good correlation between the average hourly wind speed of the sunken square and the background wind speed. The wind speeds of the sunken square and background are positively correlated, and there is a significant difference between the wind speed distributions in the two sunken squares. A comparison of the two sunken squares reveals that the shape coefficient of the sunken square has a great influence on the wind speed distribution inside the sunken square. It should be noted that, in fact, there are many factors that affect the air flow distribution of the sunken square, such as the length, width and large opening. However, we only have considered the effect of the shape of the sunken square including the height and hydraulic diameter in this study. The attenuation effect in the S-metro station is less than that of the F-metro station, and the attenuation effect increases with the shape coefficient of the sunken square.

The shape coefficient of the sunken square  $\omega$  is defined as,

$$\omega = \frac{D}{H} \quad (4)$$

where  $D$  is the hydraulic diameter of the bottom surface (m),  $H$  is the height of the sunken square (m). In this study, the shape coefficient of the sunken square of the F-metro and S-metro stations are 1.73 and 4.2, respectively.

Through the hourly average wind speed of the background and sunken square in winter and summer, the relationship between  $v_s/v_o$  (the ratio of the wind speed of the background and sunken square) and the shape coefficient of the sunken square is obtained as

$$\frac{v_s}{v_o} = 0.36 + 0.17 \ln \omega \quad (5)$$

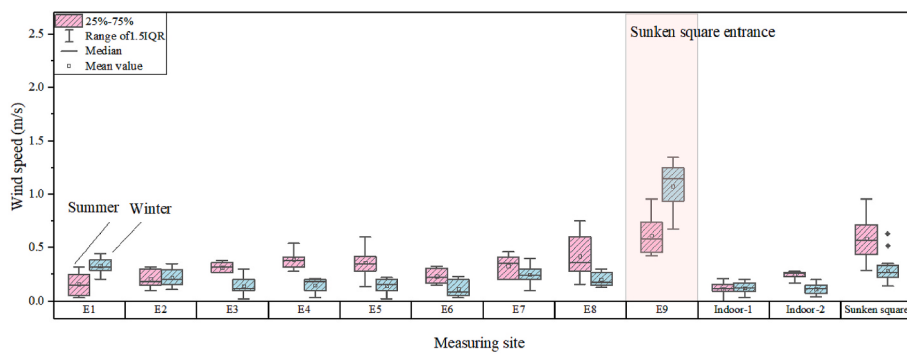
where  $v_o$  is the hourly average wind speed of the background (m/s),  $v_s$  is the hourly average wind speed of the sunken square (m/s), and  $\omega$  is the shape coefficient of the sunken square.

### 5.2. Thermal comfort of the sunken square

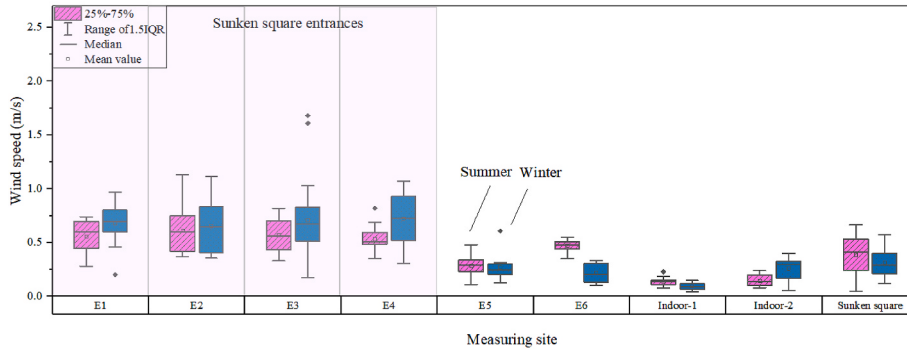
The PETs of the two sunken squares are shown in Fig. 14a. In winter, the average PET is 2 °C higher in the F-metro station sunken square than that of the S-metro station sunken square. The reason is that the relative humidity of the S-metro station sunken square is higher than that of the F-metro station sunken square, reducing the PET value more obviously. In summer, the average PET in the F-metro station sunken square is 5.1 °C higher than that of the S-metro station sunken square. The difference in PET at the two sunken squares is larger in summer than in winter because the heat radiation is strong in summer, the cooling effect is more obvious owing to the shading of trees and the self-shading effect of the surrounding environment, and the radiation effect of the surrounding walls and object surfaces is reduced.

Fig. 14b and c shows the percentage of unacceptability votes for each 1 °C of the PET bin and the second-degree polynomial fitted curve in winter and linear fitted curve in summer in the two sunken squares. A 90% acceptability was generally adopted in previous thermal comfort studies [37,38]. Thus, in this study, the acceptable range was defined such that the unacceptability rates were lower than 10%. In winter, the acceptable PET range was 17–24 °C. In summer, the acceptable PET range was less than 29.4 °C.

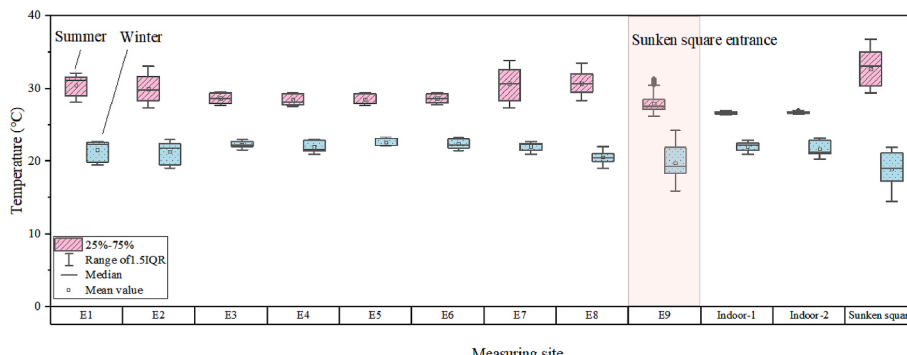
To obtain a neutral PET for different seasons, the relationship



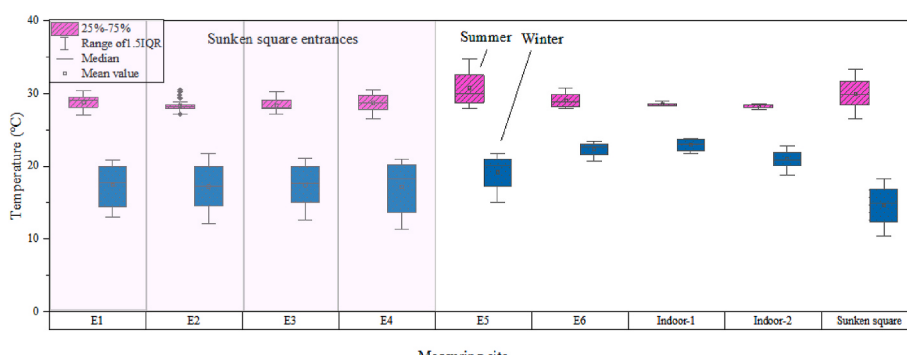
a. Wind speed at the F-metro station



b. Wind speed at the S-metro station

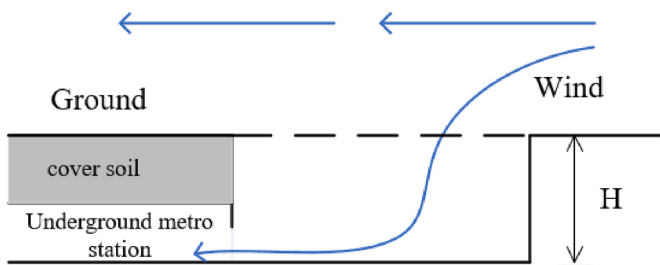


c. Temperature at the F-metro station



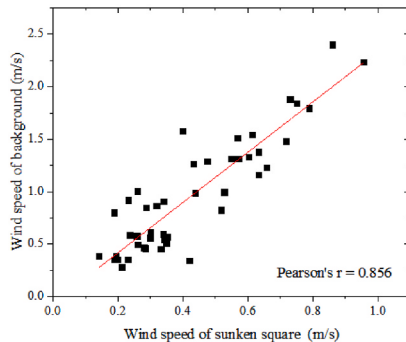
d. Temperature at the S-metro station

Fig. 11. Temperatures and wind speeds at the metro stations.

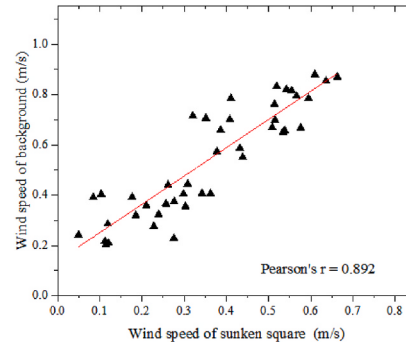


**Fig. 12.** Schematic diagram of the shape coefficient of the sunken square.

between PET and TSV was further analysed for the two sunken squares. The mean TSV (MTSV) within each PET bin, set as 1 °C for different seasons, was calculated. Fig. 14d shows the MTSV within each PET bin for different seasons. The linear regression relationships between MTSV and PET for winter and summer were obtained. The temperature at which people feel neither warm nor cool was defined as the neutral temperature. By substituting  $MTSV = 0$  in the equations above, the neutral PET was obtained: 29 and 19 °C in summer and winter, respectively. An identical PET value indicates different thermal sensations in different seasons because of the thermal adaptation.

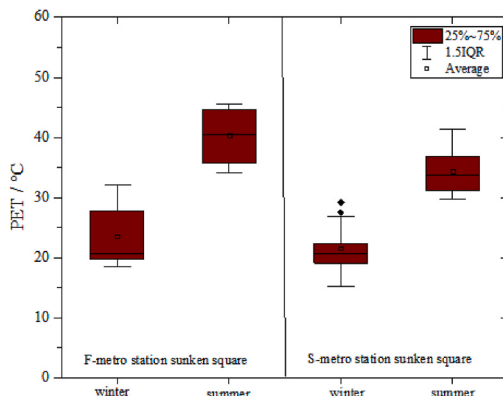


a. F-metro station sunken square

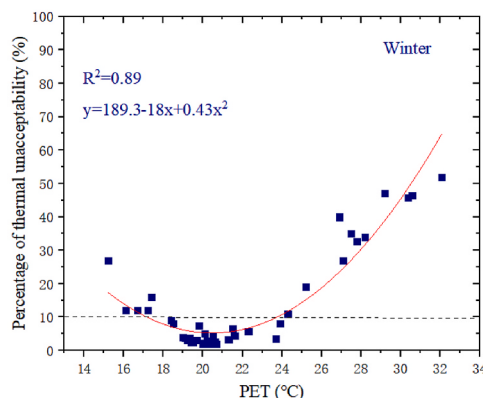


b. S-metro station sunken square

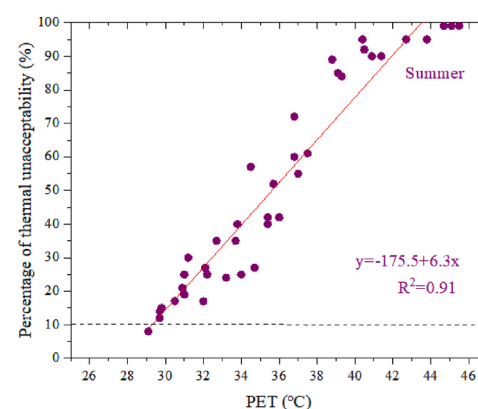
**Fig. 13.** Relationship between the wind speeds of the background and sunken square.



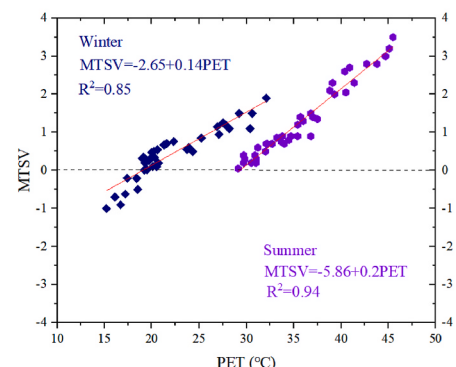
a. PET range in the sunken squares in different seasons



b. Acceptable PET range in sunken squares in winter



c. Acceptable PET range in sunken squares in summer



d. Correlations between MTSV and PET in different seasons

**Fig. 14.** PET in sunken squares.

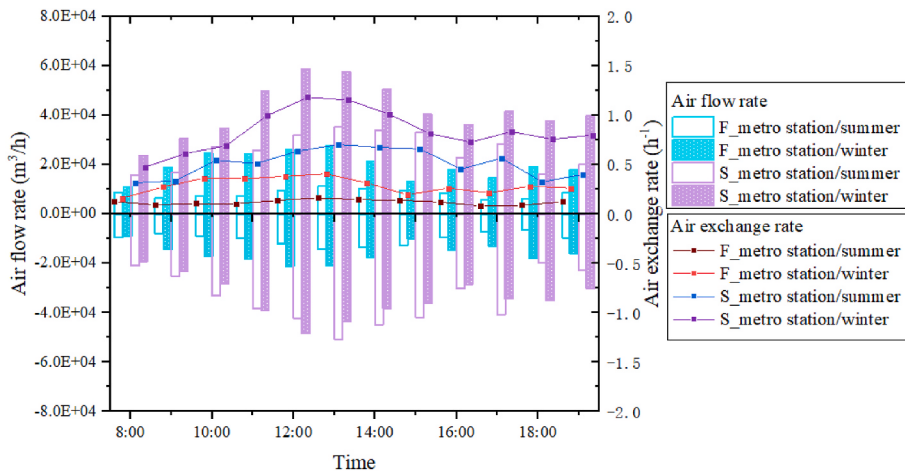


Fig. 15. Air flow rate of underground metro stations resulting from the entrances of sunken squares.

### 5.3. Air flow rate and influencing factors

According to Eqs. (1) and (2), the hourly average air flow rate and the air exchange rate of the metro stations for the sunken square entrances was estimated, as shown in Fig. 15, where '+' represents the wind direction from outdoors to indoors, and '-' represents the wind direction from indoors to outdoors. Because the supply air volume and return air volume of mechanical ventilation in the metro station is equal in winter and summer respectively according to the design standard, we believe that the air flow through the large opening of the sunken square is affected by the indoor and outdoor temperature difference and outdoor wind speed when analysis. In general, the air flow rate in the S-metro station is larger than that in the F-metro station in summer and winter because of the different shape coefficients of the sunken square, which lead to different air flow rules in the sunken squares, and the difference in the area and number of the large openings in the sunken square. In the two metro stations, the air flow rate for the sunken squares in winter is greater than that in summer. For example, in the F-metro station, the average hourly air flow rate resulting from the sunken square entrances is  $1.78 \times 10^4 \text{ m}^3/\text{h}$  in summer and  $3.58 \times 10^4 \text{ m}^3/\text{h}$  in winter. The average hourly air flow rate in winter is 1.95 times that in summer, which is promoted by the thermal pressure difference between the outdoor and indoor environments in winter; however, in summer, the internal temperature of the metro station is lower than the background weather parameter. The cold air indoors gathers inside the sunken square and metro station. In winter, the air flow entering the metro station through the sunken square entrances is greater than the air flow rate from metro station to outdoors. In summer, the pattern is reversed. This is caused by the combined interaction of temperature difference, wind direction, and the relative positions of independent entrances. For the air exchange rate, the maximum value can be as much as  $1.15 \text{ h}^{-1}$  in the S-metro station and  $0.4 \text{ h}^{-1}$  in the F-metro station in winter. In summer, the maximum values are  $0.7 \text{ h}^{-1}$  in the S-metro station and  $0.16 \text{ h}^{-1}$  in the F-metro station. Moreover, the maximum air flow rate both occur near noon in winter and summer, in order to analysis the influencing factors of the air flow rate, the partial correlation analysis method is used in this study.

To avoid the mutual influence between variables, the partial correlation analysis method is used with SPSS software when studying the influencing factors of the air flow rate. According to the significance test method for the correlation coefficient, when  $\text{sig.} = p$  and  $p \leq 0.05$ , the linear relationship is significant. When  $p \leq 0.01$ , the linear relationship is extremely significant. When  $p > 0.05$ , the linear relationship is insignificant or no linear relationship exists. Because the sunken square is a semi-underground space, its air flow characteristics differ from those of above-ground and underground buildings. For underground

Table 3

Partial correlation significance and coefficients between air flow rate of sunken square entrances and influencing factors in different seasons.

		Wind speed of background		Indoor and background temperature difference	
		p	r	p	r
F-metro station	winter	0.025	0.668	0.613	-0.172
	summer	0.018	0.694	0.019	0.689
S-metro station	winter	0.012	0.748	0.365	-0.303
	summer	0.010	0.737	0.004	0.793

buildings, the air flow rate is mainly affected by the thermal pressure difference caused by the temperature difference and wind pressure of the indoor environment and background weather parameter. For the air flow rate caused by the large openings of the sunken square entrances in this study, Table 3 shows that, in summer, the air flow rate resulting from the sunken square entrances has an obvious linear correlation with the wind speed and temperature difference between indoors and background. In winter, the air flow rate through the sunken square entrances has a positive correlation with the wind speed; however, the correlation with the temperature difference is not obvious.

## 6. Conclusions

Two representative underground metro stations in subtropical regions were studied. Through field measurement at the underground metro stations in winter and summer, the microclimates of the sunken squares of the F-metro and S-metro stations were obtained, and the effect of the sunken square on the internal environment was examined. The microclimates of different sunken squares had different characteristics, and the air flow rate of the sunken square entrances in the underground metro stations had a significant influence on the internal thermal environment. The main conclusions are as follows.

- (1) The sunken square has an attenuation effect on the background wind speed. The ratio of the average wind speed of the sunken square to the wind speed of background weather parameter at the two station was 1.3–2.3 during the measurement. The shape parameter of the sunken square has a significant influence on the wind speed inside the sunken square, and the attenuation effect increases with the shape coefficient of the sunken square.
- (2) The temperature gradually increases from bottom (1/6H) to top (6/6H) of the sunken square, and the relative humidity of the sunken square gradually decreases with height. The neutral PETs

- in the sunken squares were 29 and 19 °C in summer and winter, respectively.
- (3) The sunken square particle concentration is greater than the background particle concentration owing to the restricted air flow rate in the sunken square. The ratio of the concentration of particles with a larger particle size of the sunken square to the background is higher than that of smaller particles.
- (4) The difference in the area and number of large openings in the sunken square can influence the air flow rate in metro stations. In summer, the air flow rate through the sunken square entrances has an obvious linear correlation with the wind speed and temperature difference between indoor and background. In winter, the air flow rate through the sunken square entrances has a positive correlation with the wind speed; however, the correlation with the temperature difference is not obvious.

#### CRediT authorship contribution statement

**Jianjian Zhao:** Writing – original draft, Software, Methodology, Investigation, Data curation. **Jiankai Dong:** Supervision. **Xiaohai Zhang:** Investigation. **Yanling Na:** Resources. **Chongxu Jiang:** Resources. **Feng He:** Resources. **Qijie Cui:** Resources. **Jing Liu:** Writing – review & editing, Supervision, Resources, Methodology, Funding acquisition.

#### Declaration of competing interest

The authors declare that they have no known competing financial interests or personal relationships that could have appeared to influence the work reported in this paper.

#### Data availability

No data was used for the research described in the article.

#### Acknowledgements

This study was financially supported by China Railway Engineering Science and Technology Development Plan Project (No. 2019YY220304) “Research on Key Technologies for Internal Environmental Protection of Underground Large-scale Public Transportation Hubs”.

#### References

- [1] J. Loy-Benitez, Q. Li, P. Ifaei, et al., A dynamic gain-scheduled ventilation control system for a subway station based on outdoor air quality conditions[J], *Build. Environ.* 144 (OCT) (2018) 159–170.
- [2] V. Martins, T. Moreno, L. Mendes, K. Eleftheriadis, E. Diapouli, C.A. Alves, M. C. Minguillón, Factors controlling air quality in different European subway systems, *Environ. Res.* 146 (2016) 35–46, <https://doi.org/10.1016/j.envres.2015.12.007>.
- [3] UITP, world metro figures 8 (2018) 2018, [https://www.uitp.org/sites/default/files/ckk-focus-papers-files/Statistics Brief - World metro figures 2018V4\\_WEB.pdf](https://www.uitp.org/sites/default/files/ckk-focus-papers-files/Statistics Brief - World metro figures 2018V4_WEB.pdf).
- [4] Passi Amit, S M Shiva Nagendra, M.P. Maiya, Characteristics of indoor air quality in underground metro stations : a critical review, *Build. Environ.* 198 (April) (2021), 107907.
- [5] China Association of Subways, Annul statistics and analysis of urban railway system (In chinese), [http://wcm.cnautonews.com/pub/gdjt/hyxw/201703/t20170331\\_530367.htm](http://wcm.cnautonews.com/pub/gdjt/hyxw/201703/t20170331_530367.htm), 2016. (Accessed 10 March 2018).
- [6] T. Moreno, N. Pérez, C. Reche, V. Martins, E. de Miguel, M. Capdevila, .W. Gibbons, Subway platform air quality. Assessing the influences of tunnel vent-tiltation, train piston effect and station design, *Atmos. Environ.* 92 (2014) 461–468, <https://doi.org/10.1016/j.atmosenv.2014.04.043>.
- [7] L. Guo, Y. Hu, Q. Hu, J. Lin, C. Li, J. Chen, .H. Fu, Characteristics and chemical compositions of particulate matter collected at the selected metro stations of Shanghai, China, *Sci. Total Environ.* 496 (2014) 443–452, <https://doi.org/10.1016/j.scitotenv.2014.07.055>.
- [8] J. Han, S. bark Kwon, C. Chun, Indoor environment and passengers' comfort in subway stations in Seoul, *Build. Environ.* 104 (2016) 221–231, <https://doi.org/10.1016/j.buildenv.2016.05.008>.
- [9] Z. Yu, X. Zhu, X. Liu, Characterizing metro stations via urban function: thematic evidence from transit-oriented development (TOD) in Hong Kong[J], *J. Transport Geogr.* 99 (2022), 103299.
- [10] Shiliang SuHui ZhangMiao WangMin WengMengjin Kang, Transit-oriented development (TOD) typologies around metro station areas in urban China: a comparative analysis of five typical megacities for planning implications, *J. Transport Geogr.* 90 (2021), 102939.
- [11] P. Kumar, Sekhar Phani, C.H. Ravi, Manoranjan Parida, Identification of neighborhood typology for potential transit-oriented development, *Transport. Res.* D78 (2020), 10218.
- [12] K. Park, R. Ewing, B. Scheer, Travel behavior in TODs vs. non-TODs: using cluster analysis and propensity score matching, *Transport. Res. Rec.* 2672 (2018) 31–39.
- [13] Li You, Integration and utilization of underground street and city-A case of the sunken square in Japan and Tianfu square in Chengdu, *Urban Architecture Urban and Rural Planning and Design* 18 (2021) 382 (In chinese).
- [14] Bowen Guan, Tao Zhang, Xiaohua Liu, Performance investigation of outdoor air supply and indoor environment related to energy consumption in two subway stations, *Sustain. Cities Soc.* 41 (May) (2018) 513–524.
- [15] Wonhwa Hong, Samuel Kim, A study on the energy consumption unit of subway stations in Korea, *Build. Environ.* 39 (12) (2004) 1497–1503.
- [16] Zhangxin, Jiangyan Ma, Libin, Angui, Wenqiao Lv, Wenrong Zhang, Dehui Li, Zhangxin, Jiangyan Ma, Angui, Libin, Dehui, *Build. Environ.* 152 (2019) 87–104.
- [17] M. Hu, M. Liu, D. You, et al., Influence of train arrival characteristics on unorganized ventilation in underground subway station with platform screen doors [J], *J. Wind Eng. Ind. Aerod.* (2020) 198.
- [18] Q. Li, J. Loy-Benitez, S.K. Heo, et al., Flexible real-time ventilation design in a subway station accommodating the various outdoor PM10 air quality from climate change variation[J], *Build. Environ.* 153 (APR) (2019) 77–90.
- [19] S. Lee, M.J. Kim, J.T. Kim, et al., In search for modeling predictive control of indoor air quality and ventilation energy demand in subway station[J], *Energy Build.* 98 (Jul) (2015) 56–65.
- [20] H. Yin, C. Yang, L. Yi, et al., Ventilation and air conditioning system of deep-buried subway station in sub-tropical climates: energy-saving strategies[J], *Appl. Therm. Eng.* 178 (2020), 115555.
- [21] Yanan Liu, et al., Effects of different types of entrances on natural ventilation in a subway station, *Tunn. Undergr. Space Technol.* 105 (December 2019) (2020), 103578.
- [22] Y.H. Di, Y. Tao, J. Jiang, D.L. Li, Test and analysis of wind environment of sunken square in Xi'an area, *J. Xi'an Polytechnic Univ.* 35 (2021) 50–70 (In chinese).
- [23] Gang Han, Yueming Wen, Jiawei Leng, Lijun Sun, Improving comfort and health: green retrofit designs for sunken courtyards during the summer period in a subtropical climate, *Buildings* 11 (2021), 00413.
- [24] Caixiu Wu, Hongtuo Li, Shunxiang Zhuang, Research on the application of energy-conservation technology for metro trains, *Mod. Urban Rail Transit* 08 (2022) 33–37 (In chinese).
- [25] X. Liu, L. Lin, X. Liu, et al., Evaluation of air infiltration in a hub airport terminal: on-site measurement and numerical simulation[J], *Build. Environ.* 143 (OCT) (2018) 163–177.
- [26] K. Zhao, J. Weng, J. Ge, On-site Measured Indoor Thermal Environment in Large Spaces of Airports during winter[J], vol. 167, *Building and Environment*, 2020, 106463.
- [27] S. Shoshtarian, P. Rajagopalan, Study of thermal satisfaction in an Australian education precinct, *Build. Environ.* 123 (2017) 119–132, <https://doi.org/10.1016/j.buildenv.2017>.
- [28] T. Sharmin, K. Steemers, M. Humphreys, Outdoor thermal comfort and summer PET range: a field study in tropical city Dhaka, *Energy Build.* 198 (2019) 149–159, <https://doi.org/10.1016/j.enbuild>.
- [29] Yina Yingdi, Zhangna Dan, Zhenbin Meng, qiang Wen, Wei Jinga, Fengc LuoWei, Combined effects of the thermal-acoustic environment on subjective evaluations in outdoor public spaces, *Sustain. Cities Soc.* 77 (2022), 103522.
- [30] P. Hoppe, The physiological equivalent temperature-a universal index for the biometeorological assessment of the thermal environment, *Int. J. Biometeorol.* 43 (1999) 71–75.
- [31] Z. Fang, Z. Lin, C.M. Mak, J. Niu, K.-T. Tse, Investigation into sensitivities of factors in outdoor thermal comfort indices, *Build. Environ.* 128 (2018) 129–142.
- [32] T.P. Lin, Thermal perception, adaptation and attendance in a public square in hot and humid regions[J], *Build. Environ.* 44 (10) (2009) 2017–2026.
- [33] A. Matzarakis, F. Rutz, A. Matzarakis, F. Rutz, H. Mayer, Modelling radiation fluxes in simple and complex environments - application of the RayMan model Modelling radiation fluxes in simple and complex, *Int. J. Biometeorol.* 51 (2007) 323–334, <https://doi.org/10.1007/s00484-006-0061-8>.
- [34] A. Matzarakis, F. Rutz, H. Mayer, Modelling radiation fluxes in simple and complex environments : basics of the RayMan model, *Int. J. Biometeorol.* 54 (2010) 131–139, <https://doi.org/10.1007/s00484-009-0261-0>.
- [35] Xin Chen, Puning Xue, Lin Liu, Lixin Gao, Jing Liu, Outdoor thermal comfort and adaptation in severe cold area: a longitudinal survey in Harbin, China, *Build. Environ.* 143 (2018) 548–560.

- [36] N. Kantor, J. Unger, The most problematic variable in the course of human-biometeorological comfort assessment-The mean radiant temperature, *Cent. Eur. J. Geosci.* 3 (1) (2011) 90–100.
- [37] P. Cohen, O. Potchter, A. Matzarakis, Human thermal perception of Coastal Mediterranean outdoor urban environments, *Appl. Geogr.* 37 (2013) 1–10, <https://doi.org/10.1016/j.apgeog.2012.11.001>.
- [38] T.P. Lin, Thermal perception, adaptation and attendance in a public square in hot and humid regions, *Build. Environ.* 44 (2009) 2017–2026, <https://doi.org/10.1016/j.buildenv.2009.02.004>.